Ultrastructural Visualization of Cytoskeletal mRNAs and their Associated Proteins Using Double-Label In Situ Hybridization

Robert H. Singer, Gary L. Langevin, and Jeanne Bentley Lawrence

Department of Cell Biology, University of Massachusetts Medical School, Worcester, Massachusetts 01655

Abstract. We have been able to visualize cytoskeletal messenger RNA molecules at high resolution using nonisotopic in situ hybridization followed by whole-mount electron microscopy. Biotinated cDNA probes for actin, tubulin, or vimentin mRNAs were hybridized to Triton-extracted chicken embryo fibroblasts and myoblasts. The cells were then exposed to antibodies against biotin followed by colloidal gold–conjugated antibodies and then critical-point dried. Identification of mRNA was possible using a probe fragmented to small sizes such that hybridization of several probe fragments along the mRNA was detected as a string of colloidal gold particles qualitatively and quantitatively distinguishable from nonspecific background. Extensive analysis showed that when eight gold particles were seen in this iterated array, the signal to noise ratio was >30:1. Furthermore, these gold particles were colinear, often spiral, or circular suggesting detection of a single nucleic acid molecule. Antibodies against actin, vimentin, or tubulin proteins were used after in situ hybridization, allowing simultaneous detection of the protein and its cognate message on the same sample. This revealed that cytoskeletal mRNAs are likely to be extremely close to actin protein (5 nm or less) and unlikely to be within 20 nm of vimentin or tubulin filaments. Actin mRNA was found to be more predominant in lamellipodia of motile cells, confirming previous results. These results indicate that this high resolution in situ hybridization approach is a powerful tool by which to investigate the association of mRNA with the cytoskeleton.

THE association of messenger RNAs with cellular structures and its physiological significance has become an important area of investigation in recent years. A number of workers have shown that messenger RNA is bound to the cellular matrix since most of it is retained after detergent lysis of the cell (Lenk et al., 1977; Farmer et al., 1978; Lenk and Penman, 1979; Pudney and Singer, 1979, 1980; Fulton et al., 1980; Ben-Ze'ev et al., 1981; van Venrooij et al., 1981; Howe and Hershey, 1984; Jeffrey, 1984). More recently Bonneau et al. (1985) have shown that actin messenger RNA is associated with the cytoskeletal framework. Most of these studies employed cellular fractionation and subsequent isolation of nucleic acids. This association of mRNA with the cytoskeletal framework is most likely of physiologic significance since it appears to be required for translation (Ornelles et al., 1986).

Our laboratory has emphasized in situ hybridization as a means to investigate the expression and distribution of specific mRNA molecules within single cells. Using an in situ hybridization protocol optimized for maintaining the structural integrity of the cell and the native configuration of RNA (Lawrence and Singer, 1985), we investigated the intracellular distribution of specific mRNAs within intact cells and provided evidence indicating that mRNAs for certain cytoskeletal proteins are localized within specific regions of the cell (Lawrence and Singer, 1986). An initial approach using fluorescence detection of biotin-labeled actin DNA probes (Singer and Ward, 1982) did not involve optimized protocols and was not successful in identifying actin mRNA with a high degree of certainty.

An understanding of the molecular mechanism(s) governing this mRNA localization may well require clarification of the nature of mRNA association with the cytoskeleton, since this may be the mechanism whereby mRNAs are held in place within the cell. The investigation of mRNA–cytoskeleton association would be greatly facilitated by development of an electron microscopic in situ hybridization methodology. An ultrastructural study would provide a higher resolution view of the intracellular distribution of messenger RNA molecules particularly as it relates to the disposition of the well-studied cytoskeletal proteins.

We undertook to continue our investigation of cytoskeletal mRNAs for actin, vimentin, or tubulin since we have analyzed these molecules in situ using nonisotopic as well as isotopic detection methods (Lawrence and Singer, 1985, 1986; Singer et al., 1986, 1987; Lawrence et al., 1988). We wished to extend our observations, using biotin-labeled probes, to the resolution of the electron microscope. This resolution is possible since the detection of biotin occurs directly at the site of hybridization. Much previous work using biotin-labeled probes detected by indirect immunocytochemistry with colloidal gold–labeled antibodies has been done by B. Ham-

kalo and her associates (e.g., Hutchinson et al., 1982; Radic et al., 1987) for high resolution studies on reiterated chromosomal sequences. Recent work by Binder et al. (1986) has employed in situ hybridization using biotinated probes to lowicryl-embedded thin sections to detect mitochondrial rDNA and small nuclear RNAs using antibiotin antibodies and protein A-colloidal gold. Webster et al. (1987) have reported the detection of Po mRNA in Schwann cells. Using a whole-mount approach, we report here the detection of specific messenger RNAs using the electron microscope and their high-resolution localization within the cytoskeletal framework. Furthermore, using labeling of protein and message on the same sample, we have been able to correlate the location of these messages with actin protein but not tubulin or vimentin.

Materials and Methods

Cell Culture

Skeletal myoblasts and fibroblasts were isolated from the pectoral muscles of 12-d-old chicken embryos and cultured by standard techniques. Cells were plated in Costar six-well tissue culture plates at a density of 2 × 10^5/well containing grid assemblies: carbon-formvar coated EM grids on 22-mm circular coverslips. Grids were London 200 mesh or honeycomb gold finder types (Ernest F. Fullam, Inc., Schenectady, NY). Carbon rods and formvar were purchased from Tousimis Research Corp. (Rockville, MD). Grid assemblies were made by floating a formvar film onto glass coverslips supporting four to nine gold grids. After drying, the formvar is stabilized with a thin layer of carbon. Grid assemblies in multiwell dishes were sterilized by gamma irradiation from a Cesium-137 source in an Atomic Energy of Canada Ltd. (Kanata, Ontario, Canada). All pretreatments and washes were performed in the six-well tissue culture plates.

3-d-old cultures were extracted and fixed by a modification of the method of Lenk et al. (1977). Cells were briefly washed with isotonic buffer (0.3 M sucrose, 0.1 M NaCl, 10 mM PIPES, 3 mM $MgCl_2$, 10 μM leupeptin (Sigma Chemical Co., St. Louis, MO), 1:40 dilution of Vanadyl complex (4 mM adenosine, 0.2 M VaSO4, pH 7), then extracted for 90 s in the same buffer plus 0.5% Triton X-100 followed by another brief wash in the first buffer and then fixed with 4% glutaraldehyde in PBS, 5 mM magnesium and passed through an ethanol series (30, 50, and 70% for 5 min each). Each solution was removed by aspiration. Cells were stored in 70% ethanol at 4°C until used. To preserve microtubules, all solutions were used at room temperature and EGTA was included to eliminate calcium.

Hybridization

Cell pretreatments and hybridization conditions were the same as Lawrence and Singer (1985). Briefly, cells on grid assemblies were rehydrated in PBS with 5 mM $MgCl_2$ for at least 10 min, followed by 0.1 M glycine, 0.2 M Tris, pH 7.4 for 10 min. Afterwards cells were kept in 50% formamide, 2× SSC at 37°C for 15 min before hybridization. For ribonuclease controls, 100 μl of a 100-μg/ml solution of RNase A in 2× SSC was applied to samples for 1 h at 37°C before the 50% formamide 2× SSC prehybridization treatment. Probes used were biotinylated by nick translation (Langer et al., 1981) and were ~100–200 nucleotides in length. Cells were hybridized in buffer containing 50% formamide, 2× SSC with 100 μg/μl each of tRNA and sheared salmon sperm DNA, 1% BSA, and 1 μg/ml of probe. The nucleic acid components were heated to 90°C for 5 min in 100% formamide before adding the other components.

Each experiment consisted of at least one grid assembly per sample, so that a minimum of four grids are examined using each probe or sample treatment (e.g., RNAse treatment). Within each experiment, identical treatment with identical reagents was provided to each sample with the exception of the variable to be tested.

Each grid assembly was placed cell-side down onto a 10-μl drop of the hybridization mixture on parafilm, covered with an additional sheet of parafilm to prevent drying, and incubated for 3 h in a humidified 37°C chamber. After hybridization each coverslip was gently removed from the parafilm and placed in individual wells of a clean multiwell dish containing 2.5 ml of 50% formamide, 2× SSC, and washed on a rotating shaker for 30 min or more followed by 50% formamide, 1× SSC, and finally 1× SSC, each for 30 min. The cells were left in 1× SSC overnight at 4°C to be stained the next day with antibodies.

Antibody Staining

Grids were pretreated with 8% BSA, RNase-free (Boehringer Mannheim Diagnostics, Inc., Houston, TX) TBS, pH 7.4, for 10 min. Excess fluid was removed with bibulous paper and each grid was transferred to 100-μl drops of the primary antibody staining solution: rabbit anti-biotin (Enzo Biochem, Inc., New York, NY) diluted 1:100 in 1% BSA, 1% Triton X-100, TBS, pH 7.4 (BTTBS) and incubated for 2.5 h at room temperature. Washing was performed for 30 min on a stirring platform with 3 ml/grid of the same buffer. Grids were then drained and placed on 100-μl drops of 10-nm gold-labeled goat anti-rabbit antibody (GAR GlO; Janssen Life Science Products, Piscataway, NJ) diluted 1:100 in the same buffer and incubated at room temperature for 1–2 h followed by two 30-min washes in BTTBS and then TBS.

For double labeling of either actin, vimentin, or tubulin protein with either actin, vimentin, or tubulin mRNA, mouse monoclonals against actin, vimentin, or tubulin (Amersham Corp., Arlington Heights, IL) were included with the antibiotin first antibody and 5-nm gold-labeled goat anti-mouse (GAM IgG G5,GAM IgM G5 for antiactin, all from Janssen Life Science Products) was included with the second antibody. Antibodies were spun in a clinical centrifuge for 15 min before use.

Electron Microscopy

Cells grown and processed as described above were then critical-point dried and observed with a JEOL 100S or 100CX electron microscope at an accelerating voltage of 100 kV.

Biotination of Probe

During nick-translation with biotinated nucleotide the full-length beta actin (1.8 kb) in pBR322 is reduced to fragments that averaged <200 nucleotides per molecule. Incorporated into this probe was a biotinated analogue to thymidine (biotin-11-dUTP; Enzo Biochem). Biotin-specific activity was measured by incorporating phosphorus-labeled cytidine triphosphate into the probe simultaneously with biotinated nucleotide. Assuming the biotinated nucleotide was incorporated at 80% the rate of the equivalent unlabeled nucleotide (Langer et al., 1981) and that the total incorporation of dCTP was equimolar to TTP, we calculate that the nick-translated probe was substituted ~2–10% with biotinated nucleotides.

Results

Actin Messenger RNA Associated with the Cytoskeleton: Quantitative Considerations

Analysis by In Situ Hybridization Using Isotopically Labeled Probes. In this work, our approach has been to use whole mounts of Triton-extracted cells for in situ hybridization. We have previously described methods for obtaining morphologically well-preserved cytoskeletons from developing muscle cells (Pudney and Singer, 1979, 1980; Singer and Pudney, 1984). The permeability of the cell to the probe and antibodies is enhanced by this method and the cytoskeleton is easily visualized in its entirety because of the removal of surrounding cytosolic material which reduces contrast. Furthermore, the use of whole, critical-point dried cells allows the entire message complement to be examined; a thin-sectioning procedure would reduce the signal.

It was first necessary to determine quantitatively the extent to which actin mRNA is retained within the cytoskeletal framework of extracted cells, and to ascertain the optimal conditions for extraction and fixation. Previous work from our laboratory has shown that paraformaldehyde fixation provides some advantages over glutaraldehyde fixation for in situ hybridization to unextracted cells (Lawrence and Singer,

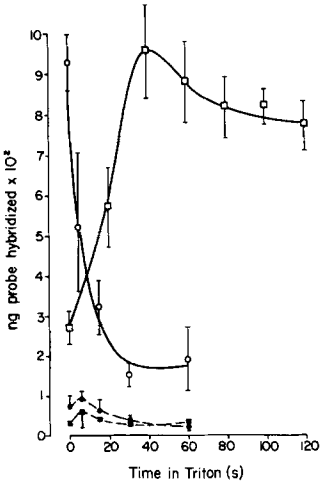

Figure 1. Quantitation of hybridization to actin mRNA in Triton-extracted cells. Cell cultures were extracted for the times indicated in 0.5% Triton, as described in Materials and Methods, and fixed for 15 min in either 4% paraformaldehyde (○) or 4% glutaraldehyde (□). Cultures were hybridized with ^{32}P-labeled probes as described and hybridization quantitated by Cerenkov radiation. Solid lines indicate hybridization with actin probe, dashed lines indicate hybridization with control pBR322.

1985). Since glutaraldehyde fixation is generally used for electron microscopic investigations of Triton-extracted cells (Pudney and Singer, 1979), we wished to compare the effects of these two fixatives. In addition we wished to determine the most appropriate extraction time for retention of mRNA and ultrastructural visualization of the cells. To determine the effect of different extraction times and fixation conditions, we employed the rapid, quantitative approach outlined in our previous work (Lawrence and Singer, 1985) where ^{32}P-labeled probes were hybridized in situ to cell cultures and then counted by Cerenkov radiation directly in a scintillation counter. This approach allows quantitation of the average amount of probe hybridized per cell.

Cytoskeletons were prepared by treatment with 0.5% Triton X-100 in isotonic buffer for varying lengths of time up to 90 s. After the treatment, the coverslips were fixed in either paraformaldehyde (4%) or glutaraldehyde (4%) for 15 min. The samples were hybridized with ^{32}P-labeled actin recombinant plasmid or with the plasmid alone as a control. The hybridization to the samples was measured and the data presented in Fig. 1. It can be seen that with paraformaldehyde-fixed cells, a progressive loss of hybridization to actin mRNA occurs as a function of extraction. Glutaraldehyde-fixed cells not treated with Triton show a much lower hybridization than paraformaldehyde-fixed cells, as has been observed previously (Lawrence and Singer, 1985; Singer et al., 1986; Singer et al., 1987). However, after short times of extraction (10–20 s), an increase in hybridization is seen where the signal approaches the level originally obtained with unextracted paraformaldehyde-fixed cells. This supports our previous conclusion, originally derived using proteinase digestion, that glutaraldehyde can presumably cross-link the nucleic acids and protein so extensively that it can be difficult for the probe to hybridize. The Triton extraction apparently removes enough soluble protein so that cross-linking does not prevent the probe access to the target molecules. Triton-extracted cells apparently have too little soluble protein left to be sufficiently fixed by paraformaldehyde for retention of mRNA during the hybridization procedure. Hence, we found glutaraldehyde to be a more appropriate fixative for in situ hybridization to mRNA in extracted cells. We chose 90 s of Triton treatment so that the maximal amount of soluble material would be removed from the cells, allowing better microscopic visualization of the mRNA bound to the cellular matrix. With this time in Triton, 70% of the actin messages are still bound to the cytoskeletal framework of chicken myoblast and fibroblast cells even after the rigorous treatment necessary for in situ hybridization. This confirms the results of Bonneau et al. (1985) using CV-1 cells. We have found that even more tubulin and vimentin messenger RNA remains bound to the cytoskeleton (90%, data not shown). Therefore, this treatment affords us a combination of mRNA retention and soluble protein extraction suitable for visualization by whole-mount electron microscopy.

Analysis by In Situ Hybridization Using Colloidal Gold Antibody Detection. The isotopic experiments above indicated a signal/noise ratio of 50:1 for hybridization to actin mRNA. This demonstrated that the extraction, fixation, and hybridization parameters used provided a strong hybridization signal appropriate to pursue further experiments using nonisotopic detection of biotin-labeled probes. The use of nonisotopic detection would be expected to reduce the signal/noise since each additional step has potential to introduce background and to diminish efficiency of detection. In initial experiments several different sources of antibiotin and gold-labeled secondary antibodies were screened, at different dilutions, to identify those which, upon visual inspection, produced the best signal. Gold-conjugated avidin was also tested, but, from the source tested, this reagent produced essentially no signal. Best results were obtained with the use of antibiotin primary antibody followed by gold-labeled secondary antibody, as described in Materials and Methods. The quantifiable nature of the gold detection particles (as with silver grains in autoradiography) afforded us the opportunity to undertake a more rigorous analysis of signal to

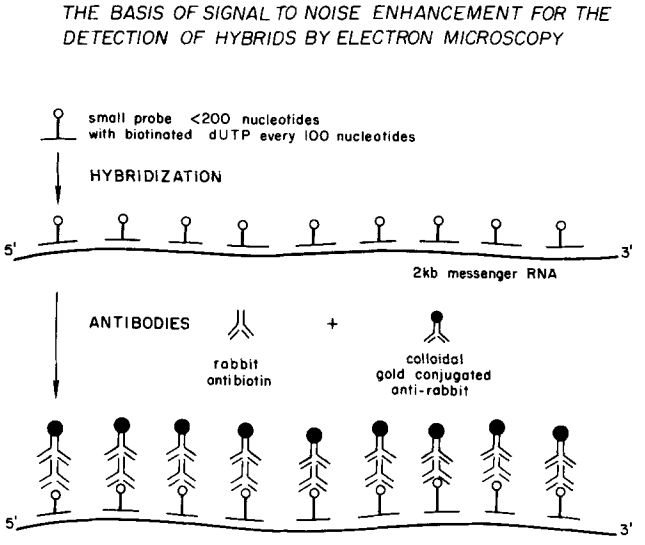

Figure 2. Schematic showing the basis for detection of bona fide signal from mRNA-biotinated DNA hybrids. The schematic presented here explains the iterative detection of a mRNA molecule using a biotinated DNA probe cut into small fragments so that each segment hybridizes independently. When the antibody detection of the biotin groups results in a string of colloidal gold particles, this distinguishes the signal from the noise generated by nonspecific sticking, either of probe or of antibody. The antibody detection of the biotin is not intended to represent the actual mode by which antibodies recognize determinants.

noise. The most straightforward approach is to count the gold particles over cells on experimental (biotinated actin probe) samples compared to that over cells on negative control samples (biotinated pBR322 probe hybridized under identical conditions). Quantitation of overall gold densities for a least 12 cells in four experiments demonstrated an average signal/noise ratio of >6:1. This was observed even though each experiment used different preparations of probes and antibodies. Therefore, >80% of the total gold particles on the actin slide represent hybridization to actin mRNA, providing good experimental material for investigation of the ultrastructural distribution of actin mRNA.

Further inspection of gold particle distribution and theoretical consideration of the labeling and detection made it apparent that individual sites of hybridization could be identified with very high confidence (>97%). This was a key element for data analysis, since our intent was to visualize hybridization with nanometer resolution at the high-magnification of the electron microscope. The strategy devised is outlined in Fig. 2, and derives from the assumption that many small probe molecules hybridize along the larger mRNA template, resulting in a tightly clustered array of gold particles qualitatively distinct from adventitious noise. Many probe molecules will hybridize at random positions dependent on the target mRNA. Subsequent detection of biotin by indirect immunocytochemistry could result in as many colloidal gold particles as biotin molecules, thereby producing an iterated array of electron-dense 10-nm images representing the templating of the target molecule. Noise, however, would have different characteristics because any nonspecific sticking of the small probe molecules or of the antibodies would be very unlikely to form an array of gold particles, since they would be individual events independent of the mRNA molecules. Hence the signal would be expected to be both quantitatively and qualitatively different than noise.

The data in Fig. 3 illustrates the results of analyzing several hundred images of these gold particles compiled from at least 10 cells (and at least two different experiments). The background levels and arrays of gold particles resulting from nonspecific sticking of probe was evaluated in control samples reacted with a biotinated pBR322 probe of the same specific activity and size as the actin probe. Antibody backgrounds were measured by the absence of probe in the protocol. The number of colloidal gold particles, as well as the number of clusters per cellular area, was significantly less in control samples reacted with biotinated pBR322 probe than with pBR 322 containing the actin insert (Fig. 3 *A*). Fig. 3 *B* shows a graph of the percentage of gold particles in each cluster size for the probe plus or minus actin sequences. It can be seen in these figures that the presence of actin cDNA in pBR 322 increases the number and percentage of colloidal gold clusters in each size category compared to control samples. The largest amount of gold particles with either probe are single and have a density of almost four gold particles per square micron for the experimental probe and about one and one-half for the control probe. As the number of particles in a cluster increases, progressively fewer clusters are found using the pBR 322 probe compared to the actin probe. It is evident that hybridization with the actin sequence yields a significant number of larger-sized (greater than six) cluster groups. This results in a proportional increase in signal-to-noise ratio (i.e., number of clusters in each size category for actin probe divided by the number for the pBR 322 probe alone) which begins at ~3:1 for individual particles and increases logarithmically to 30:1 for clusters of eight colloidal gold particles (Fig. 3 *C*). When as many as eight particles are seen in a cluster, the probability is 97% that this signal represents actin messenger RNA. It should be noted that the noise level using biotinated pBR 322 is approximately the same as when the probe is eliminated, indicating that almost all the clusters are aggregates of antibodies rather than detection of nonspecific probe sticking (data not shown). These aggregates disappear when the primary antibody is omitted indicating that the secondary antibody is not producing the clusters. Since the largest category of colloidal gold particles are singles rather than doubles, this indicates that most of the nonspecifically bound first antibody is detected by only a single secondary antibody. This may result from the large colloidal gold moiety attached which prevents more than one secondary antibody from detecting the primary antibody. These observations are reflected in the schematized drawing in Fig. 2. Finally another type of negative control sample was performed in which samples were digested in RNase A previous to hybridization. For all experiments using RNase (at least five), the amount of hybridization using the actin probe was reduced; the number of gold particles in each cluster size was decreased compared to the cells not exposed to RNase. In addition, a reduction in total gold signal as well as in cluster size was detected on several occasions when the control probe was used on the RNAse-treated cells. This may be due to the additional washing in the RNase treatment.

Analysis of Individual Clusters of Gold

When the individual clusters were examined, it became evident that there were additional qualitative differences between the mRNA probe and the control probe. In the case of the actin probe, for instance, significant numbers of clusters were found where the gold particles were not simply in an aggregate, but rather in a characteristic array with relatively constant spacing, and a linear dimension proportional to the number of gold particles involved. This is consistent with the actin probe hybridizing to a template. Examples of the visualization of individual clusters denoting hybrids are given in Fig. 4. These micrographs show the arrangement of gold particles in clusters for which the number of particles is such that it represents bonafide hybridization to an mRNA molecule. The structure of the cluster appears at times to be circular (Fig. 4, *a*, *b*, and *e*), at other times to be spiral (*c*, *d*, and *f*), and less often linear (*h*). In many cases, circular arrangements are actually spiral when examined by stereo microscopy.

Fig. 4, *e–h* shows examples of clusters denoting actin mRNA as in *a–d*, except that the sample has also been exposed to monoclonal antibodies to actin which have been detected by indirect immunocytochemistry using 5-nm colloidal gold. This allows the high-resolution visualization of both the message and its cognate protein in the same area. It is evident that actin protein is distributed throughout the area occupied by the messenger RNA. The association of the messages with the cytoskeleton can be seen clearly in these preparations. In almost all cases examined, the messenger RNA detected sits astride several filaments, very often at the base of, or along, a long, single filament the diameter of actin filaments (6 nm; see Fig. 4 *a*). In Fig. 4 *d*, actin message sits

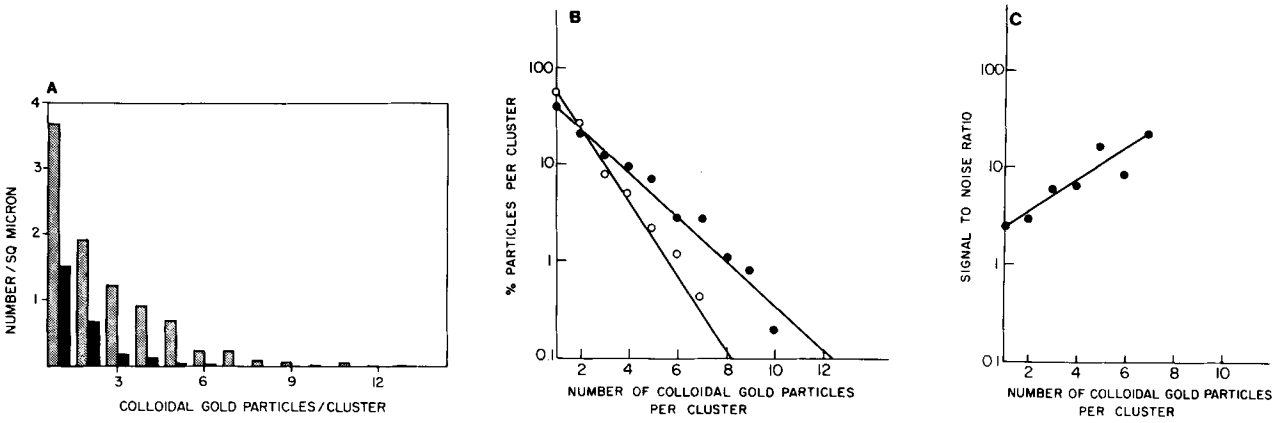

Figure 3. (*A*) Histogram showing the relationship between colloidal gold particles per unit area and the number of particles per cluster. ▨, beta-actin; ■, pBR322 or antibodies alone. (*B*) Graph showing the data in *A* as a logarithmic plot for the various clusters expressed as a percentage of total particles counted (exceeded 5,000). There were rarely any clusters of nine or more seen in the controls. ○, pBR322 probe. ●, actin probe. (*C*) Signal to noise ratio expressed as a logarithmic plot relative to numbers of colloidal gold particles per cluster. The scatter increases as the cluster size gets larger, as they represent increasingly smaller numbers. The noise level diminishes essentially to zero at cluster sizes greater than eight so that the signal-to-noise ratio becomes incalculable.

on a cellular filopodium; in Fig. 4 *g*, on a strand connecting two actin cables. When antibodies to actin are used in conjunction with the message, it is possible to see a small 5-nm particle abutting 85% of the messages within 5 nm or less (Fig. 4, *e* and *g*, *arrows*). These 5-nm particles were not seen in conjunction with the actin probe when a different (nonactin) antibody is used (see below). It is possible that this represents a nascent chain, or a recently released protein from the polyribosome. However, when messages other than actin were detected in conjunction with actin antibodies these 5-nm colloidal gold particles were also seen close to the message indicating that in the majority of the cases, it is not a nascent chain but rather an actin protein close to the message (see below).

Double-Label Visualization of Actin, Tubulin, and Vimentin Messages Correlated with Actin, Vimentin, or Tubulin Proteins

It was of interest to investigate further whether there was a functional correlation between the proximity of actin antibodies and actin messages, i.e., whether actin messenger RNA is associated specifically with its own filaments. The methodology presented here was used to explore the general relationship of cytoskeletal messages to their proteins with high resolution. We investigated cells hybridized to either a probe containing actin, vimentin, or tubulin sequences as well as the vector (pBR322) alone and used either an actin, vimentin, or tubulin antibody to correlate proximity of each of the proteins with either of the messages. Examples of some of the results are shown in Fig. 5. The vimentin antibody used was shown by electron microscopy (Fig. 5 *a*) to be specific for vimentin filaments and bundles. Fig. 5 *b* shows the detection of actin message at the lateral edge of a cell combined with vimentin antibodies and Fig. 5 *c* shows vimentin message (*arrowhead*) combined with vimentin antibodies. In this micrograph, the message is very near the nucleus, which is just off to the left. This perinuclear position, which was more common for vimentin than actin messages, is consistent with our previous observation which showed, by in situ hybridization and subsequent autoradiography, that vimentin message tends to be detected more consistently near the nucleus (Lawrence and Singer, 1986). Fig. 5 *d* shows a cell hybridized with a vimentin probe which was large (400–600 nucleotides) and shows two rows of gold particles, perhaps indicating that networks were formed as was suggested to be a result of using larger probes (Lawrence and Singer, 1985). This particular experiment showed a number of these parallel arrays of gold particles as well as cruciform and branched structures. This preparation was also exposed to antiactin antibodies represented by the small gold particles. The actin protein can be seen in close proximity to the vimentin message. Fig. 5 *e* shows a double-label experiment for tubulin mRNA and tubulin protein. Two labeled microtubules can be seen traversing the field. Tubulin mRNA is associated with other cellular material, possibly a stress fiber.

To quantitate the association of each message with each of these three filamentous proteins, the protein detected (5-nm particles) using each antibody was assessed within 5 nm of each message. The total number of messages examined in this way reflects "nearest neighbor" proximity of each protein to each message (see Table I). A great majority (88%) of all the actin or vimentin messages examined, lay close to an antibody for actin protein (at least 5 nm in distance). The tubulin messages were closely associated with actin protein 70% of the time. Nonspecific noise was generated using the vector alone, and the rare clusters were found to be near actin on significantly less occasions (46%). This may be due to the density of actin protein labeling within the cell and hence the probability that a random cluster would fall near an actin protein. However, in contrast, no more than 7.8% of these same messages lay on a filament composed of or containing vimentin or tubulin. The slightly elevated percentage obtained when tubulin and vimentin messages were correlated with their respective proteins could possibly reflect the detection of nascent chains rather than presence of a filamentous protein.

Additionally, the distance to the nearest 5-nm particle from a message was measured as an indication of the general nearness of each individual protein to either of the messages.

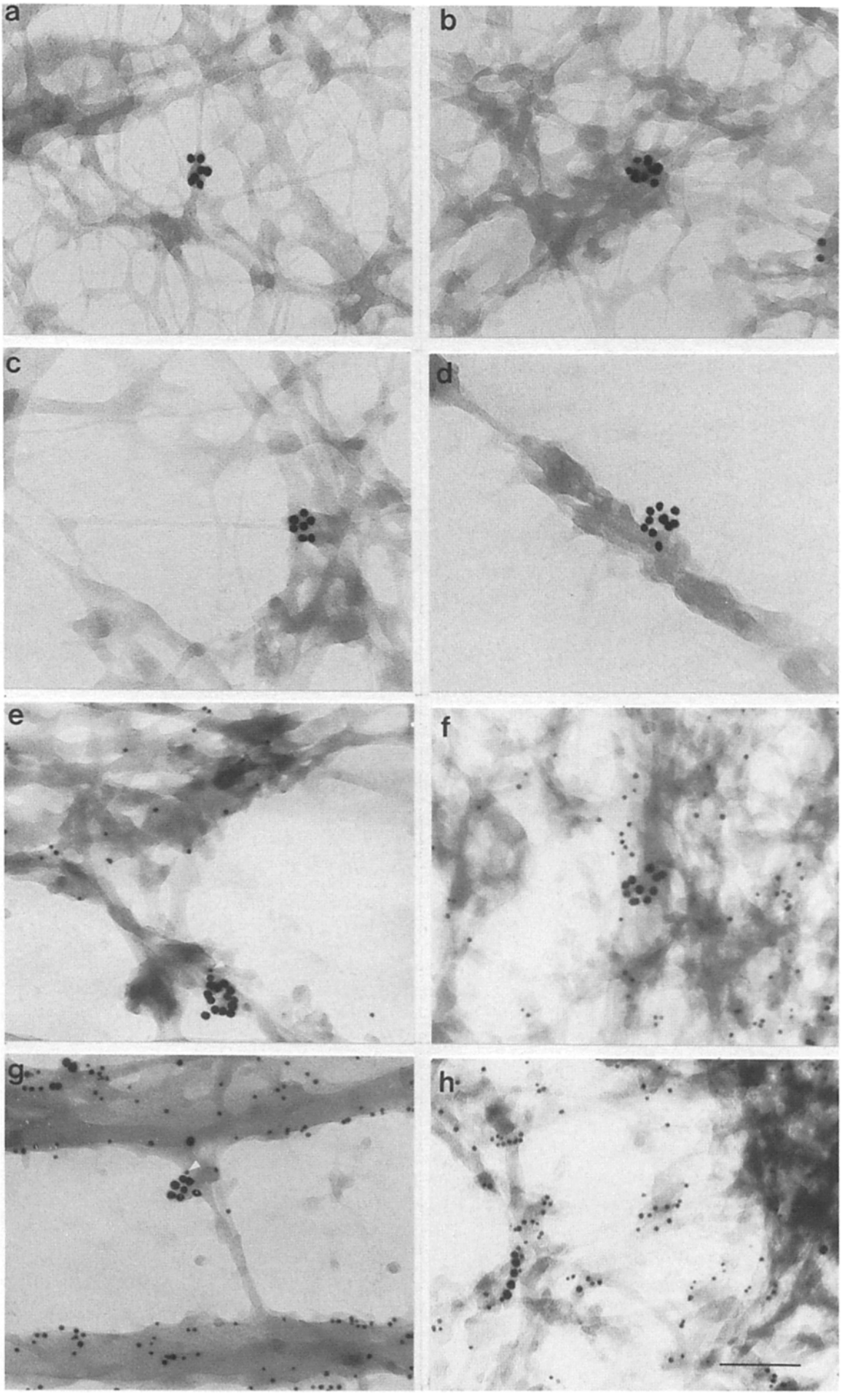
a
b
c
d
e
f
g
h

Table I. Association of Cytoskeletal Message with Cytoskeletal Proteins

Antibody	Probe			
	Actin	Vimentin	Tubulin	322
Actin	88.0 (n = 52)	89.0 (n = 27)	70.0 (n = 39)	46.0 (n = 50)
Vimentin	0 (n = 11)	7.8 (n = 51)	2.1 (n = 47)	3.7 (n = 27)
Tubulin	4.2 (n = 24)	4.8 (n = 21)	6.5 (n = 31)	3.2 (n = 31)

The frequency with which actin, vimentin, or tubulin protein is found near actin, tubulin, or vimentin message is represented as the frequency that 5-nm particles are within 5 nm of a message. Cells probed with either a vimentin, tubulin, actin, or a pBR 322 biotinated sequence and identified by the presence of more than five (10-nm) particles in a cluster were then analyzed for the nearness of 5-nm particles denoting antibodies to actin, vimentin, or tubulin. Based on the examination of duplicate samples and two different individuals to analyze the results.

The results from the analysis of several hundred negatives indicated that actin protein is as much as 40 times closer to actin, tubulin, or vimentin messages (averages <10 nm away) than either vimentin or tubulin protein is around either message (averages from 211 to 79 nm away, respectively). This absence of vimentin or tubulin protein from areas near either vimentin, actin, or tubulin mRNAs as well as the absence of messages in areas of vimentin or microtubule labeling indicate that these are unlikely to be the cytoskeletal component with which these mRNAs associate or by which it is localized. Conversely, actin protein is more likely to be in the proximity of any of the messages examined.

Cellular Location of the Messages

To gain a perspective as to the placement of cytoskeletal messages within entire cells, as was described initially by Lawrence and Singer (1986), several cells were assembled by montage at a magnification of 25,000 (one cell occupied ~10 square feet at this magnification) and the gold clusters all marked and categorized according to cluster size. A fraction of one of these cells is represented in Fig. 6. When the complement of gold particles is calculated for the entire cell and the background level subtracted for each cluster size, an approximation of 900 actin messages is obtained for this cell. When only "high confidence" messages are examined (i.e., greater than six particles per cluster, denoted by stars in Fig. 6), these are more concentrated in the lamellipodia of the cell (65% of the messages). Two cells, analyzed for hybridization to tubulin and vimentin mRNAs showed a perinuclear localization (65% of the messages), consistent with previous work cited above. Two smaller cells analyzed for actin mRNA showed similar localization to the first cell, although the message count was approximately half (~400 actin mRNAs per cell).

Discussion

This work reports the visualization of messenger RNA molecules within the cytoskeletal framework using double-label in situ hybridization and subsequent electron microscopy. The confidence in this interpretation is made possible by the iterative detection of colloidal gold-conjugated antibodies characteristic of a bona fide hybridization signal, compared to the nonspecific sticking of DNA probe or of the antibodies. It illustrates the high resolution capabilities of the biotinated nonisotopic analogue of dUTP originally described by Langer et al. (1981), since the biotinated probe is detected close to the site of hybridization unlike isotopic labeling where the detection occurs at a site distant from the actual hybridization (see also, ultrastructural detection of biotinated probes by Hutchinson et al., 1982; Binder et al., 1986; Webster et al., 1987).

The visualization of the mRNAs reported here is distinct from single-copy detection since it represents only one of many messages that are present in high abundance in the cell. A low abundance message would be difficult to detect, and hence this is a high resolution, but not a high sensitivity approach.

Do the colloidal gold clusters represent the detection of individual messenger RNA molecules? We believe each cluster corresponds to an individual messenger RNA. The evidence for this is as follows. First, the analysis of cluster sizes is consistent with a single molecular target. If messages were in the form of "packets" of more than one message, we would not expect to see colinear arrangements of gold particles but rather clumps of gold particles. Furthermore, the expected number of antibody molecules that would fit along a probe hybridizing to a 1.8-kb message at approximately one every 50 nucleotides (based on 150 Å between antigen-binding sites) would be as much as 36. In fact we rarely detected clusters this large of gold particles consistent with our detection of smaller portions of single molecules. Finally, the use of a probe for the much larger myosin heavy chain mRNA (5.9 kb) results in significantly larger clusters (Silva et al., 1989), consistent with the single mRNA as target hypothesis.

Second, the curvilinear conformation of the clusters in Triton-extracted cells is consistent with a templating by a target comprising a single strand of nucleic acid, such as would occur during hybridization. This conformation of messenger RNA has been suggested previously by the work of Chua et al. (1976) where ribosomes were seen to be packed in "hexagonal arrays" in tissues subjected to standard electron microscopic protocols. Recent work by Christensen et al. (1987) shows that membrane-bound ribosomes have almost the exact conformation even in the diameter of the circle formed as shown by the messenger RNAs visualized in this work, and suggests that there may be an association between the 3′ and 5′ ends of the message. Although cytoskeletal messages would be expected to be associated with nonmembrane-bound polyribosomes, our similar observations of the struc-

Figure 4. Sampler of actin mRNA hybrids and actin protein simultaneously detected by 5- and 10-nm colloidal gold antibodies and visualized in the electron microscope. (*a–h*) Various conformations of hybridized mRNAs seen in association with the cytoskeleton. (*a*, *c*, and *g*) mRNAs associated with vertices of filaments. (*b* and *e*) Ring configurations. (*c*, *d*, and *f*) Coiled configurations. (*e*, *g*, and *h*) Antibody staining detected within 1 nm of the messages (*small, white arrowheads in e and g*). (*d*) Coiled mRNA hybrid on a cable that was within an extracted lamellipodium. Bar, 100 nm.

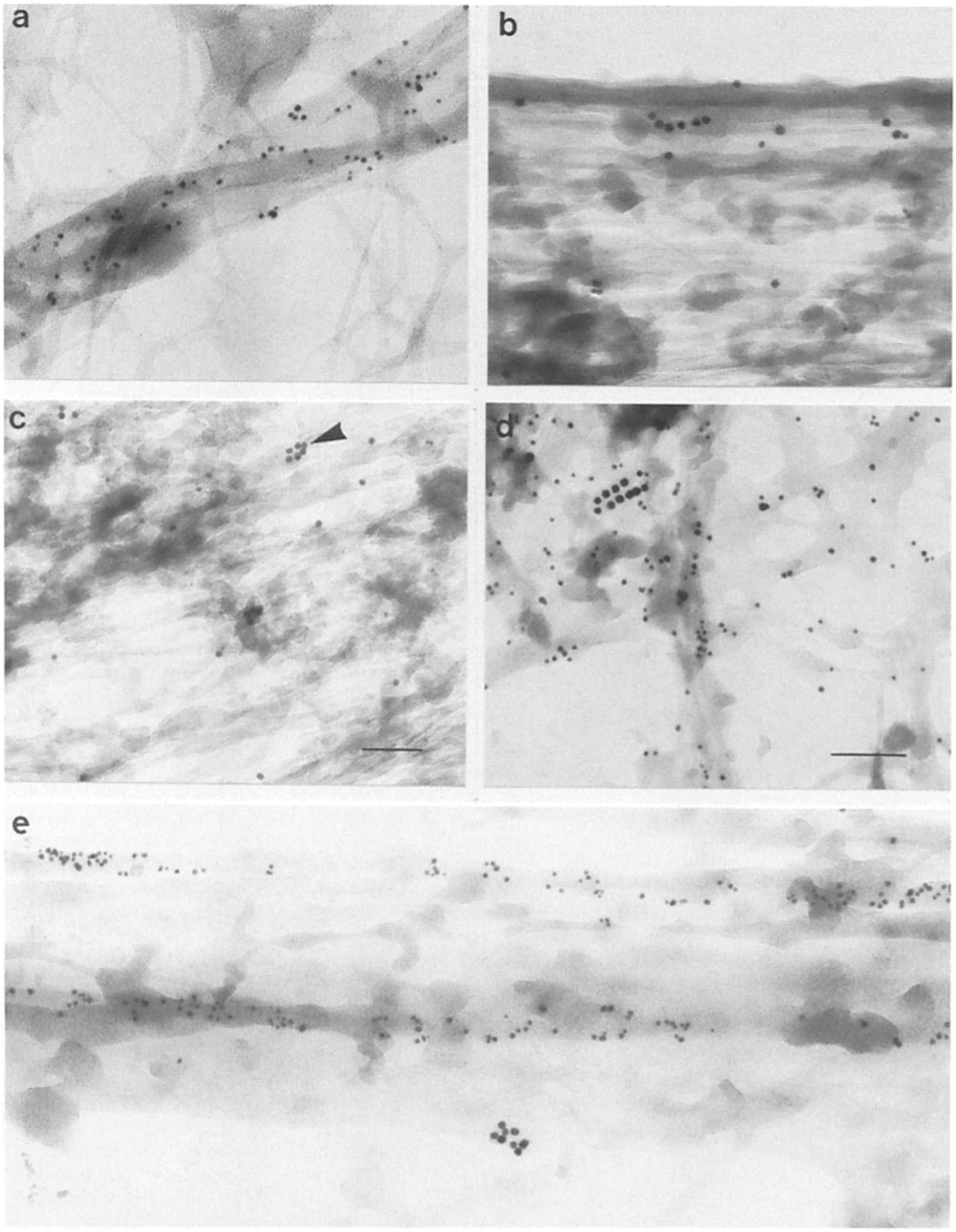

Figure 5. Double labeling in situ hybridization to detect messages with various proteins and visualized by electron microscopy. (*a*) Antivimentin antibodies detected with 5-nm colloidal gold secondary antibodies, staining a cytoplasmic vimentin cable (originated from the nucleus). (*b*) Beta-actin mRNA hybrid in a cell also stained with antivimentin antibodies detected with 5-nm colloidal gold. (*c*) Vimentin mRNA hybrid (*arrowhead*) adjacent to nucleus (not shown) in a cell stained also with antivimentin antibodies. (*d*) Vimentin mRNA hybrid in a cell also stained with antiactin antibodies. (*e*) Tubulin mRNA hybrid in a cell also stained with antitubulin antibodies. Bar, 100 nm.

ture of the hybridized messages supports this possibility. The mRNA may have this conformation imposed on it by the nature of its attachment, for instance to a helical filament.

Finally, we have counted the number of actin messages within a few specific cells, after examination of the cell in its entirety at a magnification of 25,000 and obtained for one cell ~900 actin messages (two other cells averaged 400). When compared to the results of Lawrence and Singer (1985)

Figure 6. Montage of a cell after hybridization to biotinylated actin cDNA probe and detection by indirect immunocytochemistry. A fraction of a cell is shown here, after reduction from a magnification of 25,000. The triton extraction reveals the cytoskeletal filament system, in particular, the leading edge, or lamellipodium. Clusters of six particles and greater are denoted by stars. Less than six particles are denoted by circles. Bar, 2 μm.

where an average of ~1,200 messages per cell were detected isotopically, it appears that this high resolution methodology is reasonably efficient in detecting individual messages, after correcting for the 70% of the actin messages retained after Triton extraction.

We have described in a previous work (Lawrence and Singer, 1986) that the distribution of actin messenger RNA is toward the periphery of the cell, preferentially in those regions involved in cell motility, such as lammellipodia. In the work presented here on Triton-extracted cells, we have noted similar concentrations of actin mRNA at these same sites. Reconstruction of entire cells by montage elucidated the message distributions throughout the cell and confirmed the above reference (~65% of the messages in these peripheral regions). Conversely only 35% of tubulin or vimentin messages were found in lamellipodia. The finding that messenger RNAs are not only bound to the cytoskeletal matrix in some way (see introduction of article), but are also localized to a specific region of this cellular compartment implies that a mechanism(s) of attachment exists which allows for specificity as to where on the cytoskeleton specific mRNAs are bound. The mechanism(s) governing the association of mRNAs with the cytoskeleton may be related to the mechanism(s) whereby specific mRNAs are concentrated in discrete cellular regions. Hence, the work presented here using double-labeling techniques for simultaneous detection of mRNA and protein is relevant for understanding both of these mechanism(s) by suggesting the association of cytoskeletal mRNAs with actin containing structures and the lack of association with the vimentin or tubulin containing structures. The proximity of actin protein to the cytoskeletal messages suggests that microfilaments are most likely to interact with these messages. Alternatively, the messages may interact with some actin-associated protein(s). Because of the ubiquity of actin throughout the cytoplasm, the probability that a probe will stick within 5 nm of microfilaments, based on random chance, is significant (46%). However, the probability is greater (70–89%) that mRNA for vimentin, actin, or tubulin will be near actin microfilaments. Furthermore, we searched vimentin filaments and microtubules for indication of message association and found a significantly lower association (<7.8%). Because of the diffuse and weak nature of the monoclonal antibody labeling, it was difficult to unequivocally identify microfilaments or vimentin fibers, although microtubules were more easily identified. These results suggest that it is unlikely that vimentin or tubulin are the cytoskeletal components with which the majority of their messages is directly associated. Their association with actin protein, as judged by antibody labeling, is strengthened by

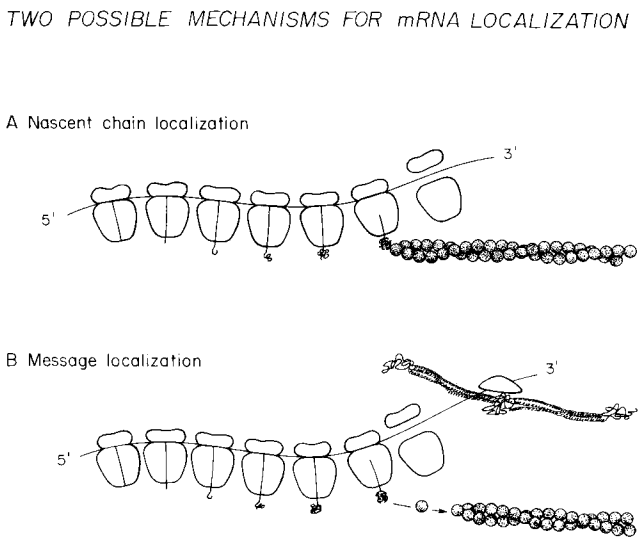

Figure 7. Scheme by which cytoskeletal messenger RNAs may be associated with the cytoskeleton and localized to particular filaments and to regions of the cell. (*A*) The mRNA becomes associated with the cytoskeleton due to the affinity of its nascent chain with a polymerizing filament, e.g., actin nascent chains may have an affinity for actin filaments. (*B*) The message associates to a filament system through a sequence on the mRNA (e.g., on the 3′ end of the message), possibly in association with a ribonucleoprotein complex. Translation results in a higher concentration of the synthesized protein around the site of attachment of the message to the filament. Evidence presented in this work indicates that while *A* may be true for actin message, *B* is more likely for vimentin, tubulin, and is also possible for actin message.

the observation that many of these messages are associated with what appear to be 6-nm filaments. This is further supported by previous work from several laboratories which investigated the association of polyribosomes with the cytoskeleton by either fractionation methods or direct visualization by electron microscopy and suggested that they were associated with microfilaments rather than intermediate filaments or microtubules (Bloemendal et al., 1979; Pudney and Singer, 1979; Lenk et al., 1979; Toh et al., 1980; Traub and Nelson, 1982; Ramaekers et al., 1983; Bird and Sells, 1986). Recent work by Ornelles (1986) indicates that cytochalasin, an actin-disrupting agent, displaces mRNA from the cytoskeleton. Isaacs and Fulton (1987) have indicated a cotranslational assembly of nascent myosin heavy chains with the cytoskeleton which is disrupted by cytochalasin. Further ultrastructural work in conjunction with additional approaches should clarify the message–cytoskeletal relationship still further (e.g., polyclonal antibodies to identify smaller actin or vimentin filaments or other actin associated proteins, or use of cytoskeletal perturbing drugs).

The possible mechanisms for specific localization of an mRNA, which have been discussed in a previous publication (Lawrence and Singer, 1986), involve targeting to a cellular region either by the nascent chain or by a nucleotide sequence on the mRNA itself (see Fig. 7). If vimentin or tubulin mRNAs are associated with actin, this would suggest that their attachment was not via an affinity of the nascent chain for its homopolymer (Fig. 7 *A*) although alternatively the nascent chain may have an affinity for actin filaments. Previous work has suggested that messenger RNA itself is attached directly to the cytoskeleton even after dissociation of the polyribosomes (Lenk et al., 1977; Cervera et al., 1981) a result consistent with the interpretation that the nascent chain is not involved in the association. Since vimentin or actin messages are concentrated in distinct regions of the cell (e.g., vimentin mRNA around the nucleus and actin mRNA in lamellipodia; Lawrence and Singer, 1986), how could this be possible if they are both associated with microfilaments? Possibly, some combination of the two proposed mechanisms exists (e.g., actin by Fig. 7 *A* and vimentin by Fig. 7 *B*), or possibly an initial role of the nascent chain in localization of the message followed by an attachment of the message to the nearest actin filament. Nonetheless the methodology employed in this work allows a direct approach toward dissecting the role of cytoskeletal elements in message association or localization. Presumably refinements in this methodology will clarify these problems further. For instance, development of a thin-sectioning approach to in situ hybridization will allow even greater ultrastructural resolution (Silva et al., 1989).

We would like to thank Elayn Byron and Linda Dill for manuscript typing and John McNeil, Sandy Marks, III, Carol Villnave, and Shirwin Pockwinse for technical help. Probes were the 1.8-kb beta-actin clone obtained from Don Cleveland, the E8 vimentin clone from Bruce Paterson and Zandra Zehner (750 bp), and the alpha and beta tubulin clones from Paul Dobner. Fred Silva contributed useful discussions. Some of the material in this work was presented in poster and abstract form in the 1986 meetings of the American Society for Cell Biology.

Supported by grant HD18066 from National Institutes of Health to R. H. Singer and J. B. Lawrence.

Received for publication 8 February 1988 and in revised form 10 January 1989.

References

Ben-Ze'ev, A., M. Horowitz, H. Skolnik, R. Abulafia, O. Laub, and Y. Aloni. 1981. The metabolism of SV40 RNA is associated with the cytoskeletal framework. *Virology.* 111:475–487.

Binder, M., S. Tourmente, J. Roth, M. Renaud, and W. Gehring. 1986. In situ hybridization at the electron microscopic level: localization of transcripts on ultrathin sections of lowicryl K4M-embedded tissue using biotinated probes and protein A-gold complexes. *J. Cell Biol.* 102:1646–1653.

Bird, R., and B. Sells. 1986. Cytoskeleton involvement in the distribution of mRNP complexes and small cytoplasmic RNAs. *Biochim. Biophys. Acta.* 868:215–225.

Bloemendal, H., E. Benedetti, F. Ramaekers, I. Dunia, M. Kibbelaar, and A. Vermorken. 1979. Is the cytoskeleton-plasma membrane complex involved in lens protein biosynthesis? *Mol. Biol. Rep.* 5:99–103.

Bonneau, A. M., A. Darveau, and N. Sonenberg. 1985. Effect of viral infection on host protein synthesis and mRNA association with the cytoplasmic cytoskeletal structure. *J. Cell Biol.* 100:1209–1218.

Cervera, M., G. Dreyfuss, and S. Penman. 1981. Messenger RNA is translated when associated with the cytoskeletal framework in normal and VSV-infected HeLa cells. *Cell.* 23:113–120.

Christensen, A. K., L. Kahn, and C. Bourne. 1987. Circular polysomes predominate on the rough endoplasmic reticulum of somatogenes and mammiotropes in the rat anterior pituitary. *Am. J. Anat.* 178:1–10.

Chua, N.-H., G. Blobel, P. Siekeivitz, and G. E. Palade. 1976. Periodic variations in the raio of free to thylakoid-bound chloroplast ribosomes during the cell cycle of *Chlamydomonas reinhardtii. J. Cell Biol.* 71:497–514.

Farmer, S. R., A. Ben-Ze'ev, B. J. Benecke, and S. Penman. 1978. Altered translatability of messenger RNA from suspended anchorage-dependent fibroblasts: reversal on cell attachment of a surface. *Cell.* 15:627–637.

Fulton, A. B., K. W. Wan, and S. Penman. 1980. The spatial distribution of polyribosomes in 3T3 cells and the associated assembly of proteins into the skeletal framework. *Cell.* 20:849–857.

Howe, J. G., and J. W. B. Hershey. 1984. Translational initiation factor and ribosome association with the cytoskeletal framework fraction from HeLa cells. *Cell.* 37:85–93.

Hutchinson, N. J., P. R. Langer-Safer, D. C. Ward, and B. A. Hamkalo. 1982. In situ hybridization at the electron microscope level: hybrid detection by autoradiography on colloidal gold. *J. Cell Biol.* 95:609–618.

Isaacs, W., and A. B. Fulton. 1987. Co-translational assembly of myosin heavy chain in developing cultured skeletal muscle. *Proc. Natl. Acad. Sci. USA.* 84:6174–6178.

Jeffrey, W. R. 1984. Spatial distribution of messenger RNA in the cytoskeletal framework of Ascidian eggs. *Dev. Biol.* 103:482–492.

Kost, T. A., N. Theodorakis, and S. H. Hughes. 1983. The nucleotide sequence of the chick cytoplasm beta-actin gene. *Nucleic Acids Res.* 11:8287–8301.

Langer, R. R., A. A. Waldrop, and D. C. Ward. 1981. Enzymatic synthesis of biotin-labeled polynucleotides: novel nucleic acid affinity probes. *Proc. Natl. Acad. Sci. USA.* 78:6633–6637.

Lawrence, J. B., and R. H. Singer. 1985. Quantitative analysis of *in situ* hybridization methods for the detection of actin gene expression. *Nucleic Acids Res.* 13:1777–1799.

Lawrence, J. B., and R. H. Singer. 1986. Intracellular localization of messenger RNA for cytoskeletal proteins. *Cell.* 45:407–415.

Lawrence, J. B., R. H. Singer, C. A. Villnave, J. L. Stein, and G. S. Stein. 1988. Intracellular distribution of human histone mRNAs in W138 cells studied by in situ hybridization. *Proc. Natl. Acad. Sci. USA.* 85:463–467.

Lenk, R., L. Ransom, Y. Kaufmann, and S. Penman. 1977. A cytoskeletal structure with associated polyribosomes obtained from HeLa cells. *Cell.* 10:67–78.

Lenk, R., and S. Penman. 1979. The cytoskeletal framework and poliovirus metabolism. *Cell.* 10:67–78.

Ornelles, D. A., E. G. Fey, and S. Penman. 1986. Cytochalasin releases mRNA from the cytoskeletal framework and inhibits protein synthesis. *Mol. Cell. Biol.* 6:1650–1662.

Pudney, J., and R. H. Singer. 1979. Electron microscopic visualization of the filamentous reticulum in whole cultured presumptive chick myoblasts. *Am. J. Anat.* 156:321–336.

Pudney, J., and R. H. Singer. 1980. Intracellular filament bundles in whole mounts of chick and human myoblasts extracted with Triton X-100. *Tissue & Cell.* 12:595–612.

Radic, M. Z., E. Lundgen, and B. A. Hamkalo. 1987. Curvature of mouse satellite DNA and condensation of heterochromatin. *Cell.* 50:1101–1108.

Ramaekers, F., E. Benedetti, I. Dunia, P. Vorstenbosch, and H. Bloemendal. 1983. Polyribosomes associated with microfilaments in cultured lens cells. *Biochim. Biophys. Acta.* 740:441–448.

Schwartz, R. J., and K. N. Rothblum. 1981. Gene switching in myogenesis: differential expression of the chicken actin multigene family. *Biochemistry.* 20:4122–4129.

Silva, F. G., J. B. Lawrence, and R. H. Singer. 1989. Progress toward ultrastructural identification of individual mRNAs in thin section: myosin heavy chain in developing myotubes. *Tech. Immunocytochem.* In press.

Singer, R. H., and D. C. Ward. 1982. Actin gene expression visualized in chicken muscle tissue culture by using *in situ* hybridization with a biotinated nucleotide analog. *Proc Natl. Acad. Sci. USA.* 79:7331–7335.

Singer, R. H., and J. Pudney. 1984. Filament-directed intercellular contacts during differentiation of cultured chick myoblasts. *Tissue & Cell.* 16:17–29.

Singer, R. H., J. B. Lawrence, and C. Villnave. 1986. Optimization of *in situ* hybridization using isotopic and non-isotopic detection methods. *Biotechniques.* 4:230–250.

Singer, R. H., J. B. Lawrence, and R. N. Rashtchian. 1987. Toward a rapid and sensitive *in situ* hybridization methodology using isotopic and non-isotopic probes. *In In situ* Hybridization: Application to the Central Nervous System. K. Valentino, J. Eberwine, and J. Barchas, editors. Oxford University Press, New York. 71–96.

Toh, B., S. Lolait, J. Mathy, and R. Baum. 1980. Association of mitochondria with intermediate filaments and of polyribosomes with cytoplasmic actin. *Cell Tissue Res.* 211:163–169.

Traub, P., and W. Nelson. 1982. Polyribosomes are not associated with vimentin-type intermediate filaments in Ehrlich ascites tumor cells. *Hoppe-Seylers Z. Physiol. Chem.* 363:1177–1185.

van Venrooij, J. J., P. T. G. Sillekens, C. A. G. van Eekelen, and R. T. Reinders. 1981. On the association of mRNA with the cytoskeleton in uninfected and adenovirus-infected human KB cells. *Exp. Cell Res.* 135:79–910.

Webster, H. F., L. Lamperth, J. T. Favilla, G. Lemke, D. Tesin, and L. Manuelidis. 1987. Use of a biotinylated probe and in situ hybridization for light and electron microscopic localization of Po mRNA in myelin-forming Schwann cells. *Histochemistry.* 86:441–444.